AIP | Journal of Applied Physics

Correlation between charge transport and electroluminescence properties of Si-rich oxide/nitride/oxide-based light emitting capacitors

Y. Berencén, J. M. Ramírez, O. Jambois, C. Domínguez, J. A. Rodríguez et al.

Citation: J. Appl. Phys. **112**, 033114 (2012); doi: 10.1063/1.4742054

View online: http://dx.doi.org/10.1063/1.4742054

View Table of Contents: http://jap.aip.org/resource/1/JAPIAU/v112/i3

Published by the American Institute of Physics.

Correlation between charge transport and electroluminescence properties of Si-rich oxide/nitride/oxide-based light emitting capacitors

Y. Berencén,[1,a)] J. M. Ramírez,[1] O. Jambois,[1] C. Domínguez,[2] J. A. Rodríguez,[3] and B. Garrido[1]
[1]*MIND-IN2UB, Dept. Electrònica, Universitat de Barcelona, Martí i Fanquès 1, 08028 Barcelona, Spain*
[2]*Instituto de Microelectrónica de Barcelona (IMB-CNM, CSIC), Bellaterra, 08193 Barcelona, Spain*
[3]*Physics Faculty, University of Havana, San Lázaro y L, Vedado, 10400 Havana, Cuba*

(Received 28 April 2012; accepted 5 July 2012; published online 14 August 2012)

The electrical and electroluminescence (EL) properties at room and high temperatures of oxide/nitride/oxide (ONO)-based light emitting capacitors are studied. The ONO multidielectric layer is enriched with silicon by means of ion implantation. The exceeding silicon distribution follows a Gaussian profile with a maximum of 19%, centered close to the lower oxide/nitride interface. The electrical measurements performed at room and high temperatures allowed to unambiguously identify variable range hopping (VRH) as the dominant electrical conduction mechanism at low voltages, whereas at moderate and high voltages, a hybrid conduction formed by means of variable range hopping and space charge-limited current enhanced by Poole-Frenkel effect predominates. The EL spectra at different temperatures are also recorded, and the correlation between charge transport mechanisms and EL properties is discussed. © *2012 American Institute of Physics*. [http://dx.doi.org/10.1063/1.4742054]

I. INTRODUCTION

Over the past years, intensive investigations have been devoted to the development of efficient silicon-based optically active materials that would permit the photonics and electronics integration in the same chip.[1–10] Silicon-rich silicon nitride (SRSN) and silicon-rich silicon oxide (SRSO) materials have mostly been considered due to their good emission properties (under optical and electrical excitation) and compatibility with the mainstream complementary metal oxide semiconductor (CMOS) technology.[1–8] Much effort has been dedicated to improve the electroluminescence (EL) intensity as well as the efficiency of the light-emitting devices.[1–4] Published works span from those centering the attention on the material optimization in terms of the different fabrication processes,[6,7] to those that mostly focus on the electrical and EL properties.[8–10] Efficient light-emitting devices have already been demonstrated using either SRSN or SRSO films.[2,4]

In former papers, we have reported the development of metal-nitride-oxide-semiconductor light-emitting devices that we called MNOSLEDs.[9,10] A typical structure of metal-oxide-semiconductor field effect transistor (MOSFET), where the gate oxide was substituted by an oxide/nitride (ON, bi-layer) or oxide/nitride/oxide (ONO, tri-layer) gate stack was used. The photometric analysis conducted in these layers represented a proof of concept for the development of silicon-based solid state lighting.[9] Until that time, no report on the use of silicon ONO-structure in electroluminescent devices had previously been published.

Two well defined bands in the EL spectra were reported in those papers: one in the near-infrared, attributed to excitonic recombination in silicon nanocrystals (Si-ncs) embedded in the tunnel SiO_2 layer and the other in the blue-green, ascribed to Si-related defects in Si_3N_4 film. Moreover, a preliminary analysis of the charge transport mechanism as well as a correlation with the electroluminescent properties was accomplished. However, neither study of the electrical conduction nor EL dependence with temperature was reported in Ref. 9 or in Ref. 10 for the ONO-based devices to firmly confirm the proposed assertions. To gain more in-depth into the physics of these mechanisms, in this paper we present a detailed study of the charge transport and electroluminescent mechanisms as a function of temperature. The MNOSLEDs studied are driven as capacitors (light-emitting capacitors), which are simpler devices than transistors from the technological and electrical viewpoint. They are based on ONO multidielectric stack. Details of the device structure as well as of the experimental measurements are given in Sec. II. The experimental results and the analysis of the electrical and electro-optical properties are discussed in Sec. III.

II. EXPERIMENTAL DETAILS

The ONO multidielectric structures were fabricated by plasma-enhanced chemical vapor deposition (PECVD) technique on B-doped p-type ⟨100⟩ Si wafer. The layer thicknesses were measured with a Gaertner L117 ellipsometer (incident He-Ne laser wavelength of 632.8 nm). The results achieved for the ONO stack are (4.2 ± 1.6)nm (top SiO_2), (29.1 ± 3.4)nm (Si_3N_4), and (7.4 ± 2.2)nm (bottom SiO_2), respectively. A silicon excess of 19% was introduced by means of ion implantation at 30 KeV and a Si dose of 4×10^{16} atoms/cm^2, after transport of ions in matter (TRIM) simulations.[11] To lower the potential barrier height and favor the hole injection from substrate into ONO active layers, the maximum of Si ions profile is centered near the lower oxide/

a)Author to whom correspondence should be addressed. Electronic mail: yberencen@el.ub.es. Tel.: +34 93 4039175. Fax: +34 93 4021148.

nitride interface (see inset of Fig. 1(a)). Subsequently, an annealing treatment at 1000 °C for 1 h was performed to recover dielectric matrices from implantation induced defects and produces a phase separation with precipitation on Si-ncs. A semitransparent polycrystalline silicon gate electrode of 100 nm thick was deposited by low-pressure chemical vapor deposition (LPCVD) at 630 °C and highly doped with $POCl_3$ at 950 °C. The ohmic contact to the lower surface of the silicon substrate was obtained by depositing 600 nm of aluminium and subsequently annealing it at 450 °C in forming gas. The device-to-device isolation was achieved by means of shallow trench isolation (STI) technique and growing a thermal oxide of 400 nm thick in the trench. The overall process sequence used follows the standard MOS procedures, which results in the final capacitor structure, as illustrated in the inset of Fig. 1(a). The device area is 5×10^{-5} cm^2.

Light emission coming from the polysilicon region was collected with a Seiwa 888 L microscope coupled to a probe station and driven through an internal system of lens to the sensitive area of detector. EL spectra were recorded with a cryogenically cooled Princeton Instruments Spec-10-100B/LN charge-coupled device and an Acton 2300i grating spectrometer. Decay EL trace was obtained with a digital GHz oscilloscope connected to a photomultiplier (R928) and a photon counter (SR430) synchronously triggered by an Agilent 8114 A pulse generator. Spectra were corrected with the optical response of the system. The electrical characterization of the devices was accomplished with a semiconductor device analyser (Agilent B1500) and a probe station (Cascade Microtech Summit 11000) with a thermal chuck system and a Faraday cage (microchamber). All the electrical and electro-optical measurements were conducted at room temperature and at different temperatures ranging from 25 °C to 300 °C.

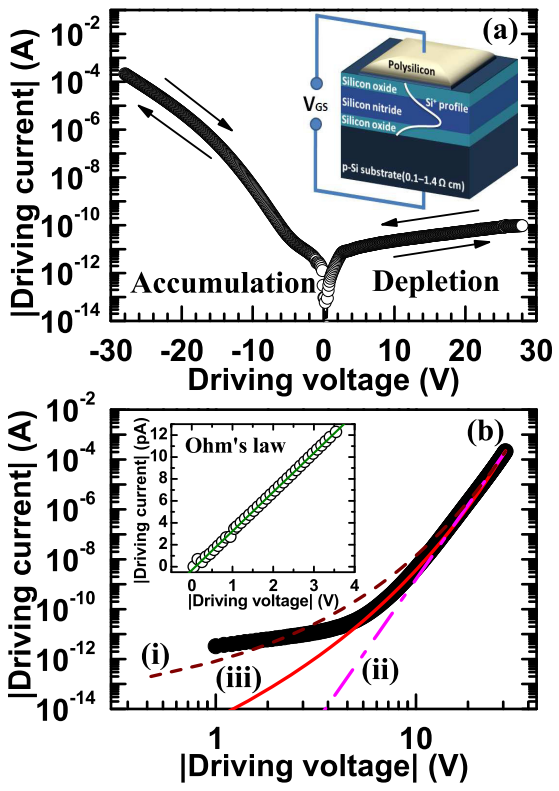

FIG. 1. (a) Typical $I(V)$ curve for light emitting capacitors based on Si-rich ONO gate stack. Inset shows a cross-sectional view and bias scheme of the devices. (b) Experimental data of $I(V)$ curve in accumulation fitted according to the different electrical conduction models listed in Table I. Schottky emission (dashed line), SCLC (dashed dotted line), and SCLC enhanced by PF effect (solid line). Inset shows the ohmic behavior at low voltages regime.

III. RESULTS AND DISCUSSION

Current-voltage characteristics $I(V)$ were first recorded at room temperature between −28 V (accumulation of the substrate, forward bias, negative voltage applied to gate) and +28 V (depletion of the substrate). A typical $I(V)$ curve is shown in Fig. 1(a). A notable rectifying behavior is seen for the devices, i.e., a very low driven current is seen in depletion regime. This feature is because of the low supply of minority carriers by the inverted substrate (electrons). It has to be also mentioned that such a depletion effect (and thus rectifying behavior) did not occur in the MNOSLED transistor structures[10] since the minority carriers can be supplied from the highly doped source and drain regions of the transistor. In the accumulation regime, a good conductivity at low and high voltages is observed. Accordingly, different conduction mechanisms (both electrode- and bulk-limited current models) were studied in detail for the $I(V)$ curves in accumulation.

Figure 1(b) shows $I(V)$ experimental data in the accumulation regime and the theoretical curves corresponding to the mechanisms and expressions listed in Table I. An ohmic dependence is observed in the inset of Fig. 1(b) for $V < \sim 3.5$ V (absolute values will be used here after). This fact could be associated with a variable range hopping-type (VRH) conduction through the localized states related with the Si-ncs.[12] The resistivity at room temperature is about 2.4×10^{16} Ω.cm at $V = 3.5$ V ($F = 0.8$ MeV/cm) which is of the same order of magnitude as that of the typical insulators.[13] Furthermore, the Schottky emission and space charge-limited current (SCLC) models are fitted to the expressions listed in Table I ranging from 3.5 V up to device breakdown (see Fig. 1(b) curves (i) and (ii), respectively). However, for this voltage range (3.5 V–28 V), the best fit is achieved with a space charge-limited current enhanced by Poole-Frenkel (PF) effect mechanism (Fig. 1(b), curve (iii)). Therefore, in this wide voltage range, the conduction is governed by a bulk-limited mechanism involving the presence of trap levels in the gap.

To confirm this assertion, before discussing the two models proposed (VRH at low voltages and SCLC enhanced by PF effect at moderate and high voltages) in more details, an Arrhenius plot has been done in accumulation regime for

TABLE I. Mechanisms of electrical conduction in insulators usually studied, and their expected current-voltage dependences.

Type of conduction	Current-voltage relation
(i) Schottky emission[14]	$I \sim \exp(aV^{1/2}/kT)$
(ii) SCLC[15]	$I \sim V$ (low fields) $I \sim V^n$ ($n > 1$, high fields)
(iii) Space charge-limited currents enhanced by Poole-Frenkel effect[16]	$I \sim V^2 \exp(aV^{1/2}/kT)$

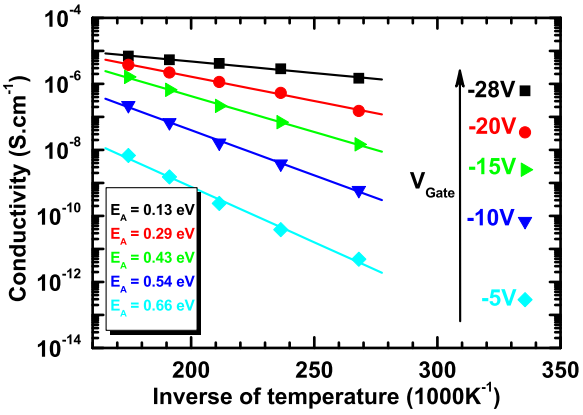

FIG. 2. Dependence between conductivity and temperature in an Arrhenius plot at different driving voltages.

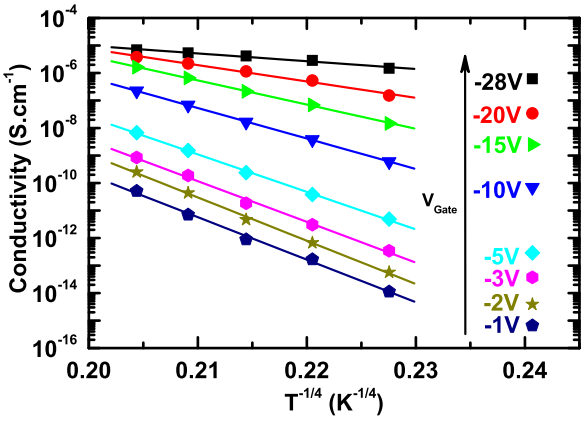

FIG. 3. Temperature dependence of the conductivity in a Mott's law plot at different driving voltages.

various driving voltages (see Fig. 2). The linear dependence observed at moderate and high voltages suggests that the existence of a thermally activated conduction mechanism (e.g., Poole-Frenkel conduction), whose average activation energy (E_A) is around 0.41 eV. This value is in close agreement with that one reported by Sze (0.64 eV) for a single stoichiometric Si_3N_4 layer.[13] In addition, further analysis of Fig. 2 shows that the activation energy decreases as the driving voltage increases. This behavior is physically acceptable as long as we consider the existence of a trap level, whose energy barrier for carrier excitation is gradually lowered by the electric field. Therefore, the activation energy E_A can be interpreted as the minimum carrier energy required to surmount the potential barrier existing between occupied and unoccupied sites.

A. Low voltages: Variable range hopping

As the conduction mechanism for silicon nitride and other dielectrics with a significant concentration of traps is mostly bulk-limited and thermally activated, we will consider the existence of a hopping-type conduction at the Fermi level located below the conduction band (at about 0.41 eV within the band gap). Thus, a VRH conduction would take place, as was originally described by Mott and Davies.[17] In such a regime, conforming to the Mott's law the conductivity is expected to vary with the temperature (T) according to $\exp(-BT^{-1/4})$, where $B = 2.06(\alpha^3/kN_F)^{1/4}$, k is the Boltzmann constant in eV, N_F is the density of states at Fermi level, and α^{-1} is the localization length characterizing the decay of the wave-function at a site. Consequently, Fig. 2 has been recalculated in a $T^{-1/4}$ representation including the low voltage range values and the resulting plot is depicted in Fig. 3. The linear behavior obtained demonstrates that the temperature dependence of the conductivity can be explained by the Mott's principle. The average value of the slope found for various driving voltages was $B = 195\text{K}^{1/4}$. Thus, if we take $\alpha = 2$ nm, which is the mean radius of our Si-ncs,[10] we find that $N_F \cong 1.12 \times 10^{18}\,\text{cm}^{-3}.\text{eV}^{-1}$. Moreover, considering that the hopping distance R and the width of the defect band ω in the VRH conduction mechanism are given by

$$R = \left(\frac{9}{8\pi\alpha N_F kT}\right)^{1/4} \quad \text{and} \quad \omega = \frac{3}{4\pi N_F R^3},$$

respectively,[17,18] we find that $R \cong 8$ nm at 300 K and $\omega = 0.42$ eV. This latter value is in agreement with the value of 0.41 eV of the Fermi level located below the conduction band. Hence, the temperature dependence of the conductivity with $\sim\exp(-BT^{-1/4})$ obtained, clearly demonstrates a pure VRH mechanism at low voltages, which is mediated by the localized states associated with the Si-ncs and/or traps distributed along the ONO multidielectric structure. By this way, we also prove the initial assumption concerning to the origin of the ohmic component. In addition, from Fig. 3, we want to stress the fact that the VRH conduction mechanism is also present at moderate and high voltages. Therefore, there will be a hybrid conduction coming from VRH and SCLC enhanced by PF effect mechanisms.

B. Moderate and high voltages: Variable range hopping + space charge-limited current enhanced by Poole-Frenkel effect

The space charge-limited current theory assumes that the trap barrier height is constant for any applied field. However, Murgatroyd[16] demonstrated that at high electric fields, the trap barrier height is lowered due to the Poole-Frenkel effect. This reduction in the barrier height increases the current level higher than that predicted by the standard space charge-limited current theory.[16,19] As can be seen in Fig. 1(b) (curve (iii)) at moderate and high voltages, the $I(V)$ curves depart from the ohmic behavior (linear) at low voltages and enter in a regime where the ratio I/V^2 proportionally raises with the square root of the voltage. Such electrical conduction feature in insulators is generally ascribed to space charge-limited current enhanced by Poole-Frenkel effect as was initially described by Murgatroyd.[16] The $I(V)$ relationship for SCLC enhanced by PF effect mechanism is given by the following expression:

$$I = \frac{9}{8}\mu\varepsilon_0\varepsilon_r S\frac{V^2}{d^3}\theta\exp\left\{\frac{0.891}{kT}\left(\frac{e^3V}{\pi\varepsilon_0\varepsilon_r d}\right)^{1/2}\right\},$$

where $\theta = N_c/N_t\,\exp(-E_A/kT)$ is the ratio of free to trapped electron concentration, N_c is the effective density of states in the conduction band, N_t is the density of traps, kT is the

thermal energy, S is the area of gate electrode, e is the electron charge, μ is the drift mobility, ε_0 is the vacuum permittivity, and ε_r is the relative permittivity of the insulator; while the factor 0.891 is derived from a numerical solution of the continuity equation. Assuming a relative permittivity of 7 and a drift mobility value of $1.25 \times 10^{-5}\text{cm}^2/(\text{V}\cdot\text{s})$, which were previously reported in similar structures,[9] we have found from fit a value of $\theta = 8.62 \times 10^{-12}$. Therefore, by using the former expression relating this parameter (θ) with N_c, N_t, E_A, and kT we are able to estimate the value of density of traps (N_t) in our Si-rich ONO multidielectric structures. Taking the typical value of $N_c \cong 10^{19}\,\text{cm}^{-3}$ (e.g., for Si, $N_c = 2.8 \times 10^{19}\,\text{cm}^{-3}$), $E_A = 0.41\,\text{eV}$ and $kT = 0.025\,\text{eV}$ we find $N_t \cong 10^{22}\,\text{cm}^{-3}$. This value is three orders of magnitude higher than for the Si non-implanted ONO structures reported by Maruyama and Shirota,[20] which suggests that the Si-ions implantation increases the density of traps in the layers irrespective of the post-annealing process. This result demonstrates and put in perspective the fact that Si-ncs could act as charge trapping centers. Obviously, the probability of occupancy of the traps depends on the Fermi-Dirac distribution function.

Summarizing the results obtained in Secs. III A and III B, we conclude that VRH is purely present at low voltages, whereas at moderate and high voltages a hybrid conduction formed by means of VRH and SCLC enhanced by PF predominates.

C. EL properties and correlation with charge transport mechanisms

Figure 4 depicts the evolution of the EL spectra as a function of temperature. It is observed that the whole visible range and part of the near-infrared are covered. Two peaks are exhibited, one centered at 1.5 eV and other broad one spanning from 2.0 eV to 3.0 eV with the maximum at 2.2 eV. The combination gives rise to a quasi-white light emission extending over the near-infrared region. The line-shape of EL spectra does not change with temperature but EL intensity for both peaks drops as the temperature increases, thus suggesting an increase of non-radiative recombination. In addition, inset of Fig. 4 shows two EL decay lifetimes (290 ns and 8.33 μs). These values were extracted from time-resolved EL measurements at room temperature by applying step-like voltage pulses to the gate with a period of 1 ms ranging from −28 V to 0 V. Moreover, both EL trace decays were well-fitted by means of a single exponential function. These lifetime values are in accordance with those recently reported by us for MNOSLED transistor structures.[10] As a result, the fastest lifetime is attributed to Si-related defects or traps present in silicon nitride matrix, likely reinforced by Si-ion implantation, whereas the lowest component corresponds to excitonic recombination due to quantum confinement effects in Si-ncs embedded into SiO_2 bottom layer.

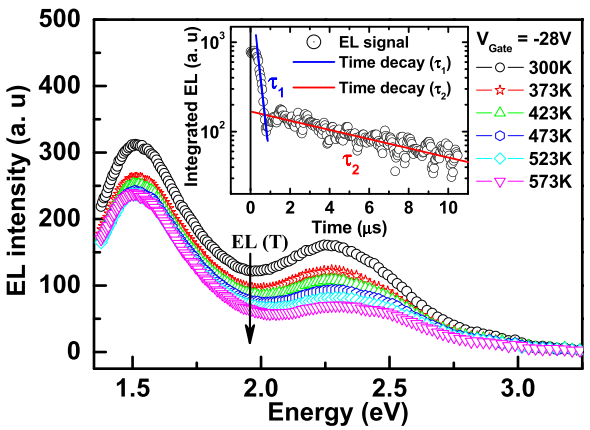

FIG. 4. Typical EL spectra for Si-rich ONO-based light emitting capacitors and their evolution as a function of the temperature. The inset shows both EL lifetimes at room temperature corresponding to Si-related defects or traps in Si_3N_4 ($\tau_1 = 290$ ns) and excitonic recombination onto Si-ncs in SiO_2 ($\tau_2 = 8.33\,\mu$s), respectively.

We have also plotted the EL spectra as a function of the driving current, as can be seen in Fig. 5. It has to be noticed that both EL peaks increase with the driving current and there are not remarkable spectral changes. This fact suggests that all luminescence species (defects and Si-ncs) are being simultaneously excited. Moreover, the inset of Fig. 5 shows a power law between the integrated EL intensity and the driving current, whose dependence is linear ($\Gamma = 1$). This observed linearity between the integrated EL and the driving current in combination with the absence of EL spectral changes suggests a univocal correlation between the injected carriers and the excited ones (i.e., Si-related defects in Si_3N_4 matrix and Si-ncs embedded into SiO_2, respectively).

The precedent results allow correlating the charge transport with the EL properties of our devices. Indeed, since the threshold voltage to get EL is around 11 V, the EL emission takes place in the range 11 V–28 V, where the electrical conduction is fully dominated by VRH and SCLC enhanced by PF effect mechanisms. Thus, electrons flow from the gate electrode through the traps present in the ONO multidielectric structures via VRH conduction and simultaneously, the trap filling process starts. This former phenomenon occurs in the voltage range from 3.5 V to 11 V before the EL emission begins. Therefore, when the electric field is strong enough ($F > 3$ MeV/cm ($V > 11$ V)) to induce the lowering of the trap barrier height, the EL emission at 2.2 eV takes place. This emission band is correlated with the PF-type ionization of the Si-related traps in Si_3N_4 matrix.[9,10] Meanwhile, the

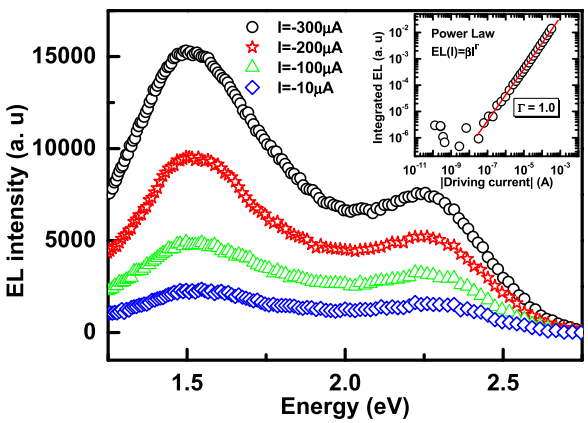

FIG. 5. EL spectra at different driving currents. Inset shows linear dependence between integrated EL intensity and driving current.

emission peak at 1.5 eV appears due to the excitonic recombination, thanks to the holes injected from the substrate into the Si-ncs embedded in the bottom layer of SiO_2,[10,21] which are recombined with the electrons injected from the gate electrode (i.e., bipolar injection).

The most distinctive difference observed between Si-rich ONO-based light emitting capacitors presented here and MNOSLEDs transistor structures previously studied lies on the electrical properties due to presence of the drain and source currents in the MNOSLEDS. As a consequence, the integrated EL intensity is higher in the transistors than the capacitors although the two EL bands are equally exhibited on both devices in accumulation regime. Nevertheless, the advantage of using MNOS capacitors instead of MNOS transistors rests on its simple structure and simple fabrication process, as well as its simplicity of analysis from the electrical and EL properties viewpoint.

IV. CONCLUSION

In summary, we have studied and correlated the charge transport and electroluminescence properties of Si-rich ONO-based light emitting capacitors from their temperature dependence. Two electrical mechanisms govern the conduction in the devices. In particular, they are variable range hopping at low voltages and variable range hopping with space charge-limited currents enhanced by Poole-Frenkel effect at moderate and high voltages, respectively. With the conduction model (VRH) at low voltages we found that the electrical conduction takes place at the Fermi level located at around 0.42 eV within the band gap, whose density of states is about $1.18 \times 10^{18}\,cm^{-3}.eV^{-1}$. Whereas at moderate and high voltages, from the SCLC enhanced by PF effect conduction model, we found that the density of the traps (N_t) is about $10^{22}\,cm^{-3}$. In addition, two EL peaks at 1.5 eV and 2.2 eV were simultaneously observed in the VRH with SCLC enhanced by PF effect conduction mechanism and correlated with the two different lifetimes noticed in the time-resolved EL measurements. Furthermore, each lifetime (290 ns and 8.33 μs) was ascribed to a PF ionization of the Si-related traps in Si_3N_4 and to an electron-hole recombination in the Si-ncs embedded in SiO_2 bottom layer, respectively. Therefore, the predominant EL excitation mechanism proceeds through the VRH and SCLC enhanced by PF effect at moderate and high voltages in which holes and electrons recombine in the Si-ncs embedded in SiO_2 bottom layer, simultaneously with the Si-related trap EL emission in the Si_3N_4 layer.

ACKNOWLEDGMENTS

The authors acknowledge funding from the Ministry of Science and Innovation (MICINN) for sample fabrication in the Integrated Nano and Microelectronics Clean Room at IMB-CNM through the ICTS access program (Project No. ICTS-NGG-31). Y.B. acknowledges financial support from the Subprograma de Formación de Personal Investigador FPI-MICINN (TEC2009-08359).

[1] J. Warga, R. Li, S. N. Basu, and L. Dal Negro, Appl. Phys. Lett. **93**, 151116 (2008).
[2] A. Marconi, A. Anopchenko, M. Wang, G. Pucker, P. Bellutti, and L. Pavesi, Appl. Phys. Lett. **94**, 221110 (2009).
[3] Z. H. Cen, T. P. Chen, Z. Liu, Y. Liu, L. Ding, M. Yang, J. I. Wong, S. F. Yu, and W. P. Goh, Opt. Express **18**, 20439 (2010).
[4] M. Perálvarez, J. Carreras, J. Barreto, A. Morales, C. Domínguez, and B. Garrido, Appl. Phys. Lett. **92**, 241104 (2008).
[5] D. Li, J. Huang, and D. Yang, Physica E **41**, 920 (2009).
[6] A. López-Suárez, J. Fandiño, B. M. Monroy, G. Santana, and J. C. Alonso, Physica E **40**, 3141 (2008).
[7] B. Shankar Sahu, F. Delachat, A. Slaoui, M. Carrada, G. Ferblantier, and D. Muller, Nanoscale Res. Lett. **6**, 178 (2011).
[8] A. A. González-Fernández, J. Juvert, A. Morales-Sánchez, J. Barreto, M. Aceves-Mijares, and C. Domínguez, J. Appl. Phys. **111**, 053109 (2012).
[9] Y. Berencén, J. Carreras, O. Jambois, J. M. Ramírez, J. A. Rodríguez, C. Domínguez, C. E. Hunt, and B. Garrido, Opt. Express **19**, A234 (2011).
[10] Y. Berencén, O. Jambois, J. M. Ramírez, J. M. Rebled, S. Estradé, F. Peiró, C. Domínguez, J. A. Rodríguez, and B. Garrido, Opt. Lett. **36**, 2617 (2011).
[11] J. F. Ziegler, J. P. Biersack, and U. Littmark, *The Stopping and Range of Ions in Solids* (Pergamon, New York, 1985).
[12] J. J. Van Hapert, Ph.D. dissertation, University of Utrecht, the Netherlands, 2002.
[13] S. M. Sze, *Physics of Semiconductor Devices*, 2nd ed. (Wiley, New York, 1981).
[14] J. O'Dwyer, *The Theory of Electrical Conduction and Breakdown in Solid Dielectrics* (Clarendon, Oxford, 1973).
[15] M. A. Lampert and P. Mark, *Current Injection in Solids* (Academic, New York, 1970).
[16] N. Murgatroyd, J. Phys. D: Appl. Phys. **3**, 151 (1970).
[17] N. F. Mott and E. A. Davies, *Electronic Processes in Non-Crystalline Materials* (Clarendon, Oxford, 1971).
[18] B. Massarani, J. C. Bourgoin, and R. M. Chrenko, Phys. Rev. B **17**, 1758 (1978).
[19] D. F. Barbe, J. Phys. D: Appl. Phys. **4**, 1812 (1971).
[20] T. Maruyama and R. Shirota, J. Appl. Phys. **78**, 3912 (1995).
[21] M. V. Fischetti, D. J. DiMaria, S. D. Brorson, T. N. Theis, and J. R. Kirtley, Phys. Rev. B **31**, 8124 (1985).